



A strategy for quality evaluation of complex herbal preparations based on multi-color scale and efficacy-oriented high-performance thin-layer chromatography characteristic fingerprint combined with chemometric method: Sanwujiao Pills as an example

Wenhan Pei^a, Yufeng Huang^b, Yuan Qu^c, Xiuming Cui^c, Liqin Zhou^d,
Hongfang Yang^d, Mingshun Zhao^d, Zhifeng Zhang^{a,***}, Fan He^{b,**}, Hua Zhou^{b,*}

^a Faculty of Chinese Medicine and State Key Laboratory of Quality Research in Chinese Medicine, Macau University of Science and Technology, Macao, 999078, PR China

^b State Key Laboratory of Traditional Chinese Medicine Syndrome, Guangdong Provincial Hospital of Chinese Medicine, Guangdong Provincial Academy of Chinese Medical Sciences, The Second Affiliated Hospital of Guangzhou University of Chinese Medicine, Guangzhou, 510006, China

^c School of Life Sciences, Kunming University of Science and Technology, Kunming, Yunnan, 650500, PR China

^d Yunnan Jinwu Black Medicine Pharmaceutical Co. Ltd., Huize, Yunnan, 654200, PR China

ARTICLE INFO

Keywords:

Quality evaluation
Herbal preparations
HPTLC fingerprint
Multi-color scale and efficacy-oriented
Chemometric method
Sanwujiao Pills

ABSTRACT

To rapidly evaluate the quality of complex herbal preparations, a new strategy was proposed based on multi-color scale and efficacy-oriented high-performance thin-layer chromatography (HPTLC) characteristic fingerprint combined with chemometric method. Firstly, effective components were screened through high-performance liquid chromatography with ultraviolet detection and evaporative light-scattering (HPLC-UV-ELSD), using multi-wavelength fusion combined with network pharmacology and molecular docking techniques. Subsequently, guided by the effective components, the targeted HPTLC characteristic fingerprint was established by multi-color scale scanning. Finally, combined with the chemometric method, the consistency of the preparation quality was evaluated, the marker components leading to quality differences were screened, and the quality control limit was established. Sanwujiao Pills (SWJPs) is a herbal preparation composed of six herbs for treating rheumatoid arthritis (RA). Through this strategy, four HPTLC characteristic fingerprints were established, they were derived from five herbs and guided by eight effective components in SWJPs. Through similarity, clustering heatmap, principal component analysis (PCA), and orthogonal partial least squares discriminant analysis (OPLS-DA), the quality distinctions among the 12 batches of SWJPs were determined. These batches were categorized into two groups based on their production time, and eight components affecting the quality of the preparation were identified. Meanwhile, the quality control threshold for SWJPs was determined based on Hotelling's T^2 and DModX methods. This strategy aims to rapidly evaluate the quality of complex herbal preparations by HPTLC and extends the application of HPTLC fingerprint chromatography for identifying herbal medicine species and activity-related

* Corresponding author.

** Corresponding author.

*** Corresponding author.

E-mail addresses: zfzhang@must.edu.mo (Z. Zhang), hefan_78@126.com (F. He), gutcmzhs@hotmail.com (H. Zhou).

<https://doi.org/10.1016/j.heliyon.2023.e22098>

Received 3 August 2023; Received in revised form 9 October 2023; Accepted 3 November 2023

Available online 8 November 2023

2405-8440/© 2023 The Authors. Published by Elsevier Ltd. This is an open access article under the CC BY-NC-ND license (<http://creativecommons.org/licenses/by-nc-nd/4.0/>).

quality detection. The proposed strategy is also helpful for the quality control of other complex herbal preparations.

1. Introduction

Herbal preparations have been used to treat diseases for thousands of years in China, demonstrating robust clinical efficacy against complex chronic diseases and garnering increasing global attention [1]. Recently, with the increasing use of herbal medicines worldwide, their quality control has been a significant concern for both health authorities and the public [2]. Herbal preparations are often made from multiple herbal medicines after extraction and processing, and hence, they have the characteristics of multiple components. The species, origin, processing method and production processes of each herbal medicine in this preparation can affect the quality consistency of herbal preparations [3], thereby influencing clinical efficacy. Therefore, establishing quality evaluation methods for complex herbal preparations and identifying components that influencing their quality have become one of the research hotspots in the field of complex herbal preparations.

Numerous methods have been developed to evaluate the quality of herbal medicines [4,5]. These include chemical fingerprint in combination with chemometrics for qualitative and quantitative analysis [6,7], integrated strategies such as “effect-compound-target-fingerprint” for discovering quality markers [8], and the “efficacy-oriented effect-constituent index” for quality control based on fingerprinting and activity detection [9,10]. Among these, chromatographic fingerprinting combined with chemometrics and efficacy assessments has gained popularity for quality evaluation. Notably, chromatographic fingerprinting is widely recognized by governmental authorities and is accepted for herbal medicines quality evaluation in many countries [11–13]. Currently, the commonly used techniques for chromatographic fingerprinting include high-performance liquid chromatography (HPLC) [14], thin-layer chromatography (TLC) [15], and gas chromatography (GC) [16], etc. Among them, high-performance thin-layer chromatography (HPTLC) is more cost-effective and more convenient than other chromatographic methods. It can realize the rapid detection of multiple batches of samples on the same thin-layer plate, especially with image analysis and stoichiometry. It has irreplaceable advantages in identifying herbal species, determining their origins, assessing processing methods, and screening bioactive components [17,18]. However, existing studies have primarily focused on individual herbal medicines, with an emphasis on qualitative identification. There are no HPTLC-related reports for quality consistency and differential component analysis of herbal preparations with complex components, and most studies have focused on using HPLC and GC methods, which are complicated to operate compared with HPTLC [14,16]. Therefore, developing an economical and rapid chromatographic fingerprinting method that can evaluate the quality of complex herbal preparations with HPTLC is challenging but meaningful.

Sanwujiao Pills (SWJPs) is a patented medicine approved by the NMPA, originating from the Sanwujiao Decoction—an herbal preparation with a history of more than 160 years of use in Yunnan, China. It is often used to treat rheumatism and rheumatoid arthritis (RA), rheumatic myositis, and hyperostosis [19,20]. Because of its good clinical efficacy, it has been approved as a therapeutic drug by NMPA and is widely used in clinical practice in China. SWJPs are prepared by decocting the following six herbal medicines in water at a high temperature and under high pressure: *Polygoni Multiflori Radix* (the root of *Polygonum multiflorum* Thunb., Heshouwu, HSW), *Aconiti Radix* (the main root of *Aconitum carmichaelii* Debx., Chuanwu, CW), *Aconiti Lateralis Radix Praeparata* (the lateral root of *A. carmichaelii* Debx., Fuzi, FZ) and *Aconiti Vilmoriniani Radix* (the root of *Aconitum vilmorinianum* Kom., Huangcaowu, HCW), *Olibanum* (the gum resin of *Boswellia carterii* Birdw., Ruxiang, RX), and *Typhonii Rhizoma* (the rhizome of *Typhonium giganteum* Engl., Baifuzi, BFZ). Among them, alkaloids are the main effective components in CW, HCW, and FZ [21], stilbene glucosides and anthraquinones are the main effective components in HSW [22], pentacyclic triterpenoids are the main effective components in RX [23], and cerebrosides are the main active components in BFZ [24]. At present, there have been only four studies on the quality control methods for SWJPs, including the TLC identification of HSW [19], HPLC fingerprints [25,26] and quantification of 2,3,5,4'-tetrahydroxy stilbene-2-O- β -D-glucoside (THSG) from HSW [27]. However, these methods can not comprehensively and objectively evaluate product quality or control the production process of the preparation. Therefore, there is an urgent need to establish a quality evaluation method capable of qualitatively identifying each herbal medicine in the preparation and objectively assessing quality consistency and variability across the different batches of the preparation.

This study proposed a novel strategy for evaluating the quality of complex herbal preparations based on a multi-color scale and efficacy-oriented HPTLC characteristic fingerprint combined with a chemometric method. This strategy has three obvious advantages: (1) The HPTLC characteristic fingerprint is based on effective components from multiple herbal medicines present in the preparation, facilitating comprehensive quality control. (2) The established characteristic fingerprints from each herbal medicine in the preparation are highly specific, eliminating interference from other herbal medicines and ensuring accuracy. (3) This strategy is rapid and economical compared to conventional HPLC and GC methods. Using SWJPs as a case study, we established the HPTLC characteristic fingerprint of five herbal medicines in the preparation, guided by eight effective components. By using this method, we evaluated the quality consistency among the 12 batches of SWJPs, identified the components responsible for quality differences in the preparation, and established quality control thresholds. To the best of our knowledge, this study is the first to evaluate the quality of a complex herbal preparation by using a multi-color scale and efficacy-oriented HPTLC characteristic fingerprint combined with a chemometric method. This strategy could be used as an efficient method to comprehensively control the quality of herbal preparations.

2. Materials and methods

2.1. Chemicals and materials

HPTLC silica gel 60 F254 (20 × 10 cm) was purchased from Merck (Darmstadt, Germany). The chemical reference substances (CRS) of emodin (EMO), physcion (PHY), 2,3,5,4'-tetrahydroxy stilbene-2-O-β-D-glucoside (THSG), emodin-8-O-β-D-glucopyranoside (EG), aloe-emodin (AE), fuziline (FZL), benzoylaconine (BAC), benzoylhyapaconine (BHA), benzoylmesaconine (BMA), 8-deacetylunaconitine (DYA), crassicauline A (CCA), 8-deacetylcrassicauline A (DCA), 3-ethyl-11-keto-β-boswellic Acid (AKBA), 11-keto-β-boswellic acid (βKBA), β-Boswellic acid (βBA), and 3-acetyl-β-boswellic acid (βABA), and β-sitosterol were purchased from Chengdu Preferred Bio-Technology Co., Ltd. (Chengdu, PR China). The herbal reference substances (HRS) of Polygoni Multiflori Radix (HSW) and Olibanum (RX) were purchased from the National Institute of Food and Drug Control (Beijing, PR China). All solvents used were of analytical or chromatographic grade and purchased from Merck (Darmstadt, Germany).

12 batches of SWJPs were obtained from Yunnan Jinwu Heiyao Pharmaceutical Co., Ltd. (Yunnan, PR China), of which 5 batches were manufactured in June 2020 (Lot: 200603, 200604, 200607, 200608, and 200609), bearing serial numbers A1 to A5; while the remaining seven batches were produced in July 2020 (Lot: 200,701–200707), with serial numbers are B1 to B7.

2.2. Preparation of sample, negative sample, HRS and CRS solutions

2.2.1. Sample, negative sample, HRS, and CRS solutions for HSW

To 4.0 g of the 12 batches of the SWJPs powder, 30 mL of water was added and sonicated for 30 min, and then filtered. The filtrate was evaporated. The residue was dissolved in 25 mL of water, shaken, and extracted twice with an equal volume of ether. The upper ether layer was collected and dried. The residue was dissolved in 1.0 mL of methanol and used as the sample solution for HSW.

The negative sample were prepared following the production process of SWJPs with the other five herbs excluding HSW, and the negative sample solution was prepared using the same method as the sample solution. For the HRS, 0.50 g HRS of HSW was processed using the same method as the sample solution for HSW. 2.0 mg of EMO and PHY, 1.0 mg of THSG CRS, and 1.0 mL of methanol were prepared a mixed CRS solution for determining the effective components in HSW.

2.2.2. Sample, negative sample, and CRS solutions for CW, HCW, and FZ

To 4.0 g of the 12 batches of the SWJPs powder, 2 mL of ammonia solution was added to wet the sample and 30 mL diethyl ether was added again. The mixture was sonicated for 30 min and filtered. The filtrate was dried and the residue was dissolved in 1.0 mL of methanol and used as the sample solution for CW, HCW, and FZ.

The negative sample were prepared following the production process of SWJPs with the other three herbs excluding CW, HCW, and FZ, and the negative sample solution was prepared using the same method as the sample solution. To BAC, BHA, and BMA CRS, isopropanol-methylene chloride (1:1) solution was added to prepare 1.0 mg/mL of the mixed CRS solution for determining the effective components in CW, HCW, and FZ.

2.2.3. Sample, negative sample, HRS, and CRS solutions for RX

To 1.0 g of the 12 batches of the SWJPs powder, 20 mL of methanol was added and sonicated for 30 min, and then filtered. The filtrate was evaporated. The residue was dissolved in 20 mL of water, shaken, and extracted with an equal volume of ether. The upper ether layer was collected and dried. The residue was dissolved with 1.0 mL of methanol and used as the sample solution for RX.

The negative sample were prepared following the production process of SWJPs with the other five herbs excluding RX, and the negative sample solution was prepared using the same method as the sample solution. 0.50 g HRS of RX was processed using the same method as the sample solution to prepare HRS solution for RX. To 0.50 mg of βBA and βABA CRS, 1.0 mL of methanol was added to make a mixed CRS solution for determining the effective components in RX.

2.3. Establishment of HPLC-UV-ELSD fingerprint with multi-wavelength fusion

HPLC-UV-ELSD with multi-wavelength fusion method was used to establish the fingerprint of SWJPs for chemical composition analysis. To this end, 2.0 g of SWJPs powder from each of the 12 batches was combined with 50 mL of methanol, sonicated for 30 min, and filtration. 25 mL of filtrate was collected and evaporated, and the residue was dissolved with 5.0 mL of methanol to generate the sample solution.

The HPLC analysis was conducted using an Agilent 1260 Infinity HPLC system (Agilent Technologies, Santa Clara, CA, USA) comprising an Agilent ChemStation software, quaternary pump, UV detector, and ELSD detector. The separation utilized a Waters XSelect CSH C18 column (4.6 × 150 mm, 5 μm), with the column temperature at 35 °C, and the injection volume of 10 μL. The mobile phases consisted of 0.1 mol/L ammonium acetate aqueous solution (A) and acetonitrile (B). The elution was developed with a flow rate of 1.0 mL/min using the following gradient elution program: 8–10 % B (0–3 min), 10–15 % B (3–11 min), 15–20 % B (11–19 min), 20–23 % B (19–23 min), 23–24 % B (23–33 min), 24–35 % B (33–37 min), 35–60 % B (37–60 min), 60–65 % B (60–75 min), 65–80 % B (75–90 min), and 80 % B (90–100 min). The multi-wavelength detection was set at 320 nm from 0 to 26 min, 235 nm from 26 to 36 min, and 254 nm from 36 to 100 min. ELSD conditions were set as follows: evaporator temperature at 50 °C, nebulizer temperature was 40 °C, and gas flow rate and PMT gain set to 1.50 SLM and 1.0, respectively.

2.4. Pharmacological network analysis

The components detected in the HPLC-UV-ELSD fingerprint were used in this study. The PubChem database (<https://pubchem.ncbi.nlm.nih.gov/>) was used to obtain their 2D structures. The 2D structures of components were imported to the Swiss Target Prediction database (<http://www.swisstargetprediction.ch/>) to screen the components targets. Through the GeneCards database (<https://www.genecards.org/>) and OMIM database (<https://www.omim.org/>), the disease-related targets were screened using the keywords “pain”, “inflammation”, “arthritis”, and “rheumatoid arthritis (RA)”.

Using the Venny 2.1.0 website (<https://bioinfogp.cnb.csic.es/tools/venny/>), the intersectional targets of SWJPs components and RA were obtained. These targets were subsequently subjected to protein-protein interaction (PPI) network analysis using the String database (<https://string-db.org/>), with a confidence threshold of 0.40. Cytoscape v3.9.1 software was used to visualize the resulting PPI network, and the CytoNCA plug-in was used to calculate the degree values of the key targets. The top six degree values in intersectional targets were selected as the key core targets of SWJPs in RA treatment.

Gene Ontology (GO) functional annotation and Kyoto Encyclopedia of Genes and Genomes (KEGG) pathway analyses were conducted for the potential targets of SWJPs in the treatment of RA using the Metascape database (<https://metascape.org/gp/index.html#/main/step1>). Criteria for significance was set at $P < 0.05$, and the resulting biological information and potential pathways were visualized using Cytoscape v3.9.1, yielding a network diagram of “SWJPs-effective components-targets-pathways”.

2.5. Molecular docking analysis

The top six key core targets identified from the PPI network diagram in Section “2.3” were selected for molecular docking with the components of SWJPs detected in the HPLC-UV-ELSD fingerprint. Firstly, the 2D structures of SWJPs’ components were minimized for structural energy and converted to 3D structures by Chem3D 20.0 software. Secondly, the protein structures of the key targets was retrieved from the RCSB PDB database (<https://www.rcsb.org/>) and imported into Pymol 2.5.4 software for dehydration and ligand separation. Finally, the AutoDock vina 1.1.2 software was used for molecular docking. The binding energy of ≤ -4.25 kcal/mol indicates a certain level of activity between the ligand and receptor protein, while a value of ≤ -5 kcal/mol suggests some degree of binding activity, and a value of ≤ -7 kcal/mol indicates strong binding activity [28,29]. The results were imported into Pymol 2.5.4 software for molecular docking visualization analysis.

2.6. HPTLC procedure

2.6.1. HPTLC of the effective components for HSW

10 μ L of the SWJPs sample solution and the negative sample solution for HSW, 5 μ L of the HRS solution for HSW, and the mixed CRS solution of EMO, PHY and THSG, were separately applied to the same HPTLC silica gel 60 F254 plate. With trichloromethane-methanol-formic acid (v:v:v = 7:3:0.5) as the mobile phase, the thin-layer plate was developed to approximately 3.5 cm, and then allowed to dry. Then, a different mobile phase consisting of petroleum ether-ethyl acetate-formic acid (v:v:v = 15:5:0.5) was used to develop the plate to about 7 cm, followed by drying. The bands were visualized under the ultraviolet light at 365 nm. Finally, the plate was sprayed with 5 % (w/v) vanillin-sulfuric acid reagent, then heated at 105 °C, and the bands were examined under sunlight.

2.6.2. HPTLC of the effective components for CW, HCW and FZ

15 μ L of the SWJPs sample solution, negative sample solution for CW, HCW and FZ, and 10 μ L of the mixed CRS solution of BAC, BHA, and BMA were separately applied to the same HPTLC silica gel plate. With n-hexane-ethyl acetate-methanol (v:v:v = 6.4:3.6:1) as the mobile phase, the thin-layer plate was pre-saturated for 30 min in the chromatography cylinder filled with ammonia vapor. It was then developed to approximately 9 cm and allowed to dry. The bands were examined under sunlight after spraying with the Dragendorff reagent.

2.6.3. HPTLC of the effective components for RX

15 μ L of the SWJPs sample solution and the negative sample solution for RX, 2 μ L of the HRS solution for RX, and 10 μ L of the mixed CRS solution of β Ba and β ABA were separately applied to the same HPTLC silica gel plate. Using petroleum ether (60–90 °C)-cyclohexane-ethyl acetate-formic acid (v:v:v = 10:30:15:1) as the mobile phase, the thin-layer plate was developed to approximately 9 cm and then allowed to dry. The plate was sprayed with a 10 % (v/v) sulfuric acid-ethanol solution and heated at 105 °C until the bands were clear. The bands were then examined under sunlight.

2.7. Image and data processing of HPTLC

High-definition images of the HPTLC plate were captured using a TLC Visualizer system (CAMAG, Muttenz, Switzerland). The Chemical Fingerprint Analysis System Solution software (ChemPattern®, 2020, Beijing, China) was used for image processing and digitized chromatogram data acquisition (Version 2020, Chemmind Corp., Beijing, China).

The HPTLC images were imported into ChemPattern® (2020) software, which automatically located thin-layer development tracks of the samples, eliminated the interference bands in the negative sample solution. Next, the HPTLC images were digitally scanned with multiple color scales using UV color mode. Ultraviolet light at 365 nm was scanned with a positive color (+) channel, while visible light and UV 254 nm with a negative color (–) channel. This process converted the color information into a skeleton map based on intensity

value, enabling the integration of peak areas for each component band. The median method was used to screen the common peaks and their R_f value, and the mean method was used to calculate the eigenvalues. Finally, a Gaussian curve simulation algorithm was employed for visualization to generate the common pattern of the HPTLC characteristic fingerprint.

2.8. Validation of the HPTLC fingerprint method

The specificity, robustness, and repeatability of the method were assessed in accordance with ICH guidelines [30]. Three batches of SWJPs sample solution (B1–B3), negative sample solution, mixed CRS solution, and HRS solution from each herbal medicine were applied to the same HPTLC plate to evaluate the robustness concerning different manufacturer's HPTLC plates, temperature, and humidity. Negative sample solutions, prepared using any five herbs from the six herbs in SWJPs, were observed to assess the specificity of the method. Batch B1 was used to prepare six sample solutions repeatedly and applied to the same thin-layer plate to assess repeatability. Finally, the relative standard deviation (RSD%) of common peaks in the HPTLC fingerprint was calculated.

2.9. Chemometric analysis for quality evaluation

2.9.1. Similarity and cluster heatmap

ChemPattern® software was employed to assess the quality consistency of the 12 batches of SWJPs by similarity evaluation. The data of the common peaks in the HPTLC fingerprint from different batches of samples were standardized and compared to the common pattern of the HPTLC fingerprint of SWJPs. The angle cosine method was used to calculate the similarity of samples. Meanwhile, cluster heatmap analysis was used to cluster the 12 batches of SWJPs based on HPTLC fingerprint data with Euclidean distance and complete linkage method to determine the quality difference among SWJPs batches.

2.9.2. Principal component analysis (PCA)

PCA was utilized to reduce the dimensionality of multidimensional sample data to several principal components and determine the quality consistency and differences among samples according to the principal components. The fingerprint data from the 12 batches of SWJPs were subjected to dimensionality reduction analysis in the ChemPattern® software. The variance contribution rate of each principal component was obtained, and the grouping of SWJPs from different batches was predicted to analyze the quality consistency

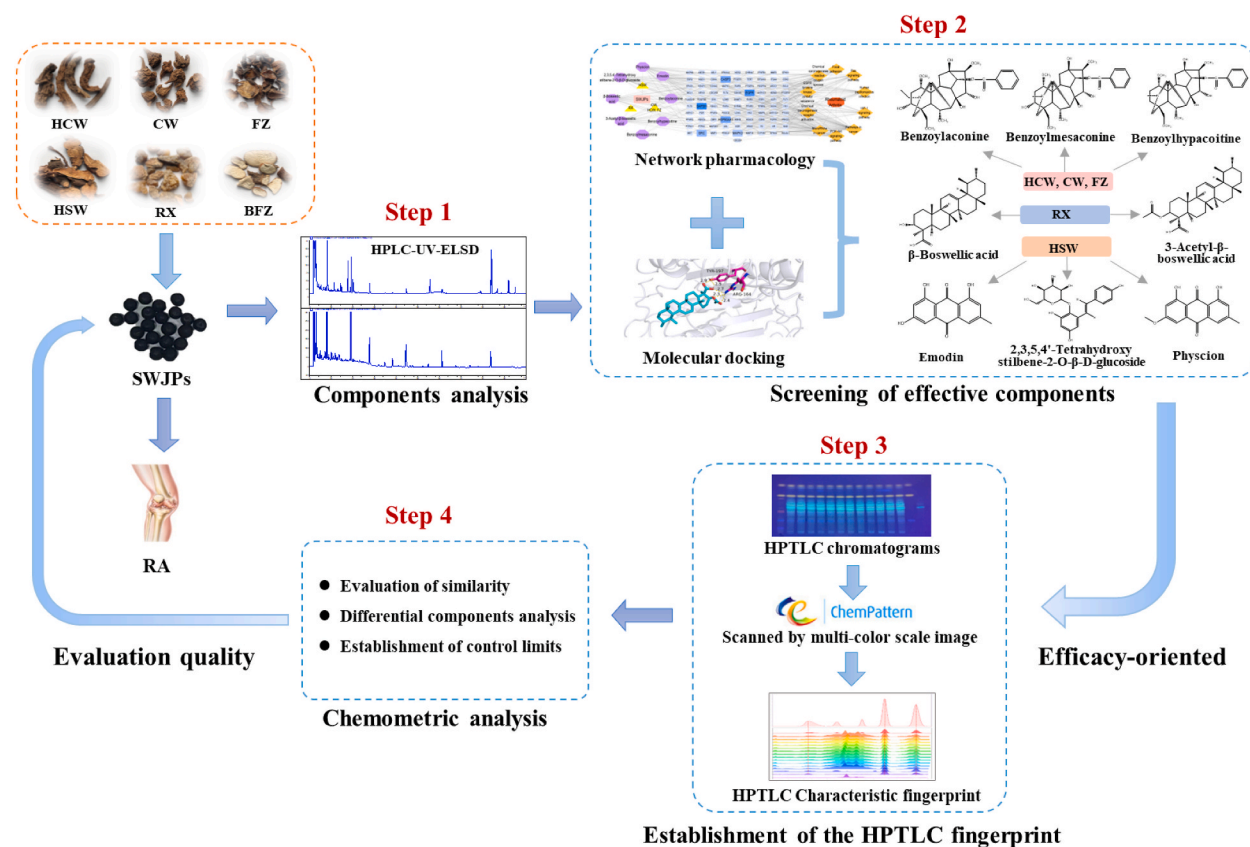


Fig. 1. The strategy for quality evaluation of complex herbal preparations based on multi-color scale and efficacy-oriented HPTLC characteristic fingerprint combined with chemometric methods: Sanwujiào Pill as an example.

of the preparation. Finally, Hotelling's T^2 and DModX control charts were created to monitor the quality of different batches of samples.

2.9.3. Orthogonal partial least-squares discrimination analysis (OPLS-DA)

To further screen the marker components responsible for the quality differences in SWJPs, the common peak data from HPTLC fingerprints of different batches of SWJPs were subjected to supervised OPLS-DA using the SIMCA-P 14.1 software (Sartorius, Göttingen, Germany). Two hundred permutation tests were performed on the established OPLS-DA model to assess its validity. The variable importance in the projection (VIP) value was used to predict the components that differentiated the quality of SWJPs. These components (VIP > 1) were considered to be key factors contributing to the quality differences in SWJPs.

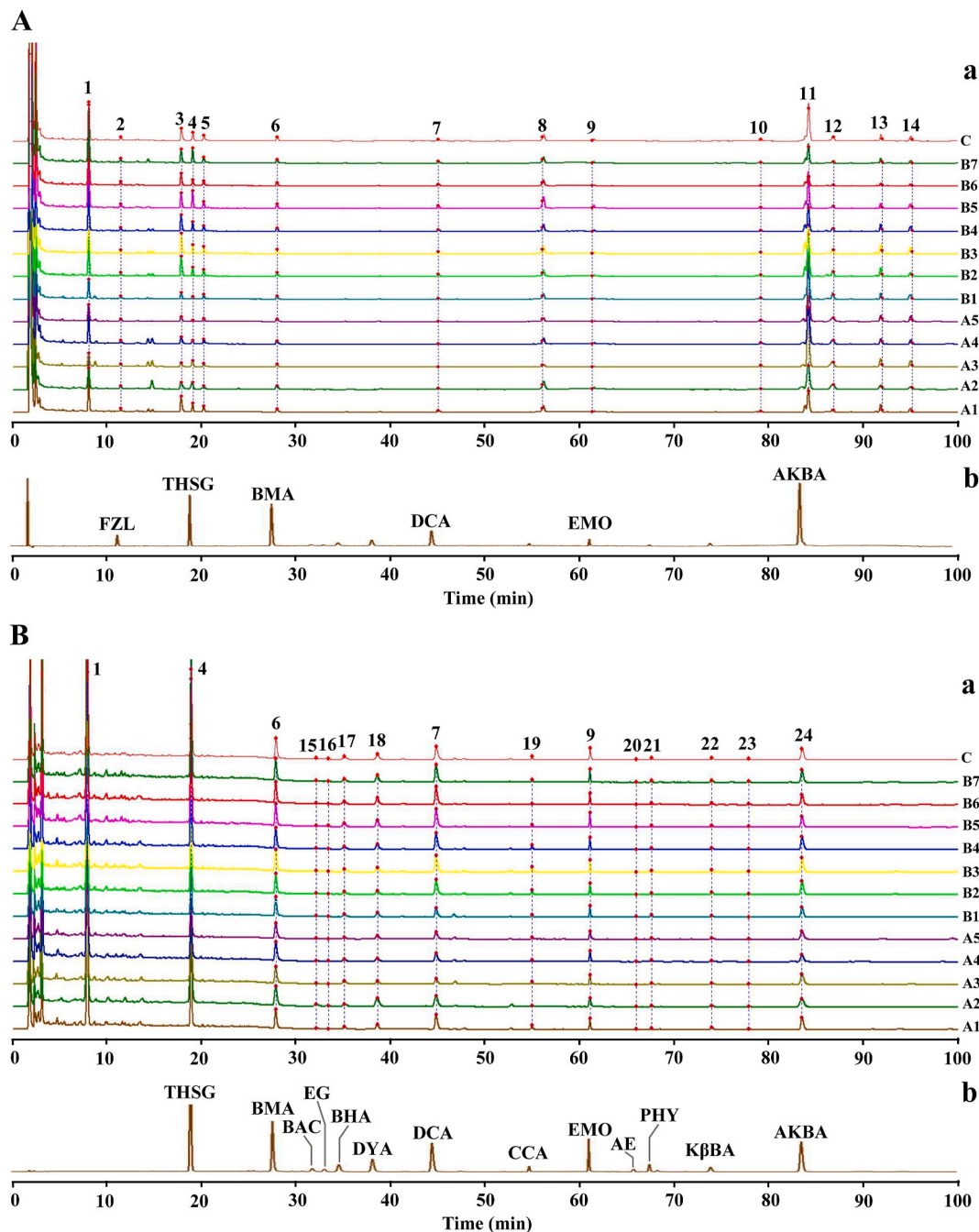


Fig. 2. HPLC-UV-ELSD fingerprints of SWJPs. (A) HPLC-ELSD fingerprint, (B) HPLC-UV fingerprint. (a) Overlay of fingerprints of 12 batches of SWJPs and reference (common pattern), (b) Chromatogram of mixed reference solution.

3. Results and discussion

3.1. Strategy for quality evaluation

A comprehensive and rapid strategy for evaluating the quality of SWJPs was proposed (Fig. 1), The steps were as follows: (1) The HPLC-UV-ELSD fingerprint with multi-wavelength fusion was established to determine the common compositions of SWJPs. (2) Effective components for the treatment of RA were screened by the pharmacological network and molecular docking technology based on the common compositions of SWJPs. (3) A specific HPTLC characteristic fingerprint was developed based on multi-color scale images and effective component orientation. This fingerprint was unique to each herbal medicine in SWJPs, eliminating negative interference from other herbal medicines. (4) Combined with the chemometrics methods, the quality consistency of the samples was evaluated, the marker components affecting the quality were identified, and the control limit for evaluating quality was established.

3.2. Analysis of HPLC fingerprint components

To identify the components in SWJPs, HPLC-UV-ELSD was performed to establish the fingerprints of the 12 batches of SWJPs with multi-wavelength fusion. The main components were anthraquinones, diterpenoid alkaloids, stilbene glycosides, and masticinic acids. Therefore, 320 nm was selected for stilbene glycosides, 235 nm for alkaloids, and 254 nm for anthraquinones and masticinic acids. At the same time, UV and ELSD detectors were used to detect the sample's UV and non-UV absorption components fully.

A total of twenty-four common peaks were obtained using ELSD and UV, and fourteen components were identified by comparisons with standard substances (Fig. 2) and UPLC-QTOF-MS/MS analysis (Fig. S1, Table S1). Additionally, three components (β BA, β ABA and β -sitosterol) were detected in the HPTLC pre-experiment for SWJPs, but were not detected by HPLC-ELSD-UV. Therefore, seventeen components in SWJPs were selected for screening the effective components in the treatment of RA (Table 1), including three anthraquinones and one stilbene glycosides from HSW, eight alkaloids from CW, HCW and FZ, four masticinic acids from RX, and one sterols from BFZ.

3.3. Identification of the effective components for treating RA

3.3.1. Screening of the key targets of components for treating RA

Through network pharmacology, we sought to identify key targets associated with the 17 components detected in SWJPs for the treatment of RA. A total of 362 targets were related to the components, 8491 targets were related to RA, and an intersection of 312 targets was observed, accounting for 3.7 % (Fig. 3A), representing potential drug targets for SWJPs in RA treatment. The PPI network and visualized PPI map of potential targets were obtained by String database and Cytoscape v 3.9.1 software (Fig. 3B), comprising 310 nodes connected with 3485 interacting lines. Based on the degree value, the top six targets were selected as the key targets for SWJPs in RA treatment, namely GAPDH, EGFR, CASP3, HSP90AA1, SRC, and MAPK3.

3.3.2. Analysis of GO function and KEGG enrichment pathway

GO functional annotation and KEGG enrichment pathway analysis were performed on the intersecting targets of the components and RA. The analysis yielded a total of 2552 GO entries, including 2121 biological processes (BP), 137 cellular components (CC), and

Table 1

Analysis results of HPLC-UV-ELSD fingerprint components in SWJPs.

NO	component	attribution of herbal medicine	
1	2,3,5,4'-tetrahydroxy stilbene-2-O- β -D-glucoside	Polygoni Multiflori Radix	
2	emodin		
3	physcion		
4	aloe-emodin		
5	emodin-8-O- β -D-glucopyranoside		
6	benzoylaconine		
		No.6-12 components all belong to Aconiti Radix, Aconiti Vilmoriniani Radix, and Aconiti Lateralis Radix Praeparata	
7	benzoylhypaconitine	Olibanum	
8	benzoylmesaconitine		
9	8-deacetylyunaconitine		
10	crassicauline A		
11	8-deacetylcrassicauline A		
12	fuziline		
13	3-ethyl-11-keto- β -boswellic Acid		
14	11-keto- β -boswellic acid		
15	β -boswellic acid		
16	3-ethyl- β -boswellic Acid		
17	β -sitosterol		Typhonii Rhizoma

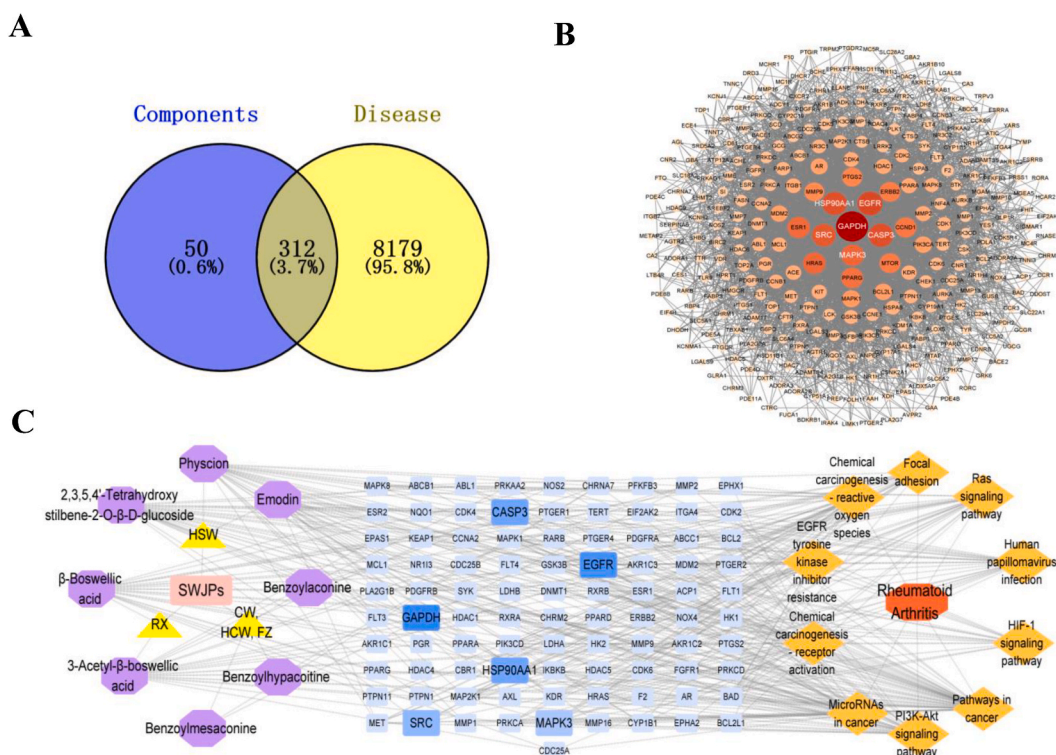


Fig. 3. Network pharmacology of SWJPs in the treatment of RA. (A) Venn diagram of the intersection targets between components and RA, (B) The PPI network of the potential targets of SWJPs, and (C) “SWJPs-effective components-targets-pathways” networks.

294 molecular functions (MF). Response to hormones, cellular response to nitrogen compounds, and protein phosphorylation were involved in BP. Membrane raft, membrane microdomain, and protein kinase complex were involved in CC. Phosphotransferase activity, alcohol group as acceptor, alcohol group as acceptor, kinase activity, and protein kinase activity were involved in MF. The KEGG enrichment analysis produced 194 items ($P < 0.05$), elucidating the involvement of numerous pathways in SWJPs’ treatment of RA. Predominant pathways included cancer-related pathways, PI3K-Akt signaling pathway, microRNAs in cancer, and chemical carcinogenesis – reactive oxygen species.

3.3.3. Analysis of “SWJPs-effective components-targets-pathways” network

The top 10 KEGG pathways were selected to draw the “SWJPs-effective components-targets-pathways” network map combined with the effective components and “drug-disease” intersection targets of SWJPs (Fig. 3C). As shown in Fig. 3C, Eight effective components act on the above 10 signaling pathways that play an important role in the treatment of RA. The network involved a total of 91 targets, among which GAPDH, HSP90AA1, SRC, EGFR, CASP3, and MAPK3 were the key targets of SWJPs in treating RA. It was consistent with the targets screened by the method in Section 3.3.1. This network shows that SWJPs mainly play a role in treating RA through pathways in cancer, PI3K-Akt signaling pathway, microRNAs in cancer, and other pathways.

3.3.4. Screening of the effective components by molecular docking

Molecular docking simulations were conducted to assess the binding capabilities of seventeen components in Section 3.2 with the six key targets screened in Sections 3.3.1 and 3.3.2. It evaluated the success rate based on their binding energy values. The results

Table 2
Combinative energy value of the effective components of SWJPs in the treatment of RA.

Effective components	GAPD (H)	EGFR	CASP3	HSP90AA1	SRC	MAPK3
THSG	-9.9	-5.2	-8.0	-6.8	-3.9	-8.2
EMO	-9.7	-5.9	-8.1	-8.0	-3.1	-8.2
PHC	-9.6	-5.7	-7.9	-7.2	-3.9	-9.2
BAC	-8.0	-5.8	-7.1	-6.6	-5.0	-8.0
BHA	-8.5	-5.6	-7.1	-6.4	-4.5	-8.4
BMA	-7.6	-5.7	-6.9	-6.3	-4.3	-7.7
βBA	-8.6	-5.9	-8.4	-7.3	-4.0	-8.9
βABA	-8.5	-6.2	-9.1	-7.2	-3.7	-8.3

indicated that eight components in SWJPs exhibited favorable binding energies with key targets of RA (Table 2), including BAC, BHA, BMA, THSG, EMO, PHY, β BA, and β ABA (Fig. 4). They had strong binding ability to HSP90AA1, EGFR and CASP3 target proteins. Notably, all their binding energies were ≤ -5 kcal/mol, especially for GAPDH and MAPK36 with a binding capacity of ≤ -7 kcal/mol. Collectively, these findings suggest that the selected effective components correlated strongly with RA. Additionally, these components were found to be present in high concentrations, making them detectable by HPTLC in SWJPs and thus laying the foundation for the study of HPTLC fingerprints.

3.4. Analysis of the HPTLC chromatograms

The four HPTLC chromatograms were generated for the five herbal medicines in SWJPs, based on the eight effective components obtained from the above screening (Fig. 5). Among these components, EMO, PHY, and THSG belong to anthraquinones and stilbene glucosides, respectively, originating from HSW [22]. Moreover, BAC, BHA, and BMA are diterpenoid alkaloids found in CW, HCW and FZ [21], β BA and β ABA are pentacyclic triterpenoids present in RX [23].

To better detect the effective components on the thin-layer plate, the suitable detection wavelengths and derivative reagents that were sensitive to these components were identified. Because the absorption wavelength of anthraquinones is UV 365 nm [31] and vanillin is the identification reagent of glucosides [32], UV 365 nm and vanillin were selected to examine the thin-layer plate for HSW. The Dragendorff reagent is an identification reagent of alkaloids [33], and 10 % (v/v) sulfuric acid-ethanol solution is the identification reagent for pentacyclic triterpenoids [34]. Thus, the two reagents were selected as derivative reagents for alkaloids from CW, HCW, FZ, and pentacyclic triterpenoid from RX.

The four HPTLC chromatograms for the five herbal medicines in SWJPs indicated consistent chromatographic behavior of 12 batches of SWJPs, with clear and stable bands. Notably, the chromatograms revealed specific components in each herbal medicine that could be distinguished from their respective negative sample solutions.

Furthermore, this study introduced a novel method to simultaneously detect stilbene glucosides and anthraquinones in HSW using twice-development method. This study solved the problem that only one component could be detected by TLC in most herbal preparations containing HSW. Thus, it enabled comprehensive quality control for the multiple components of HSW.

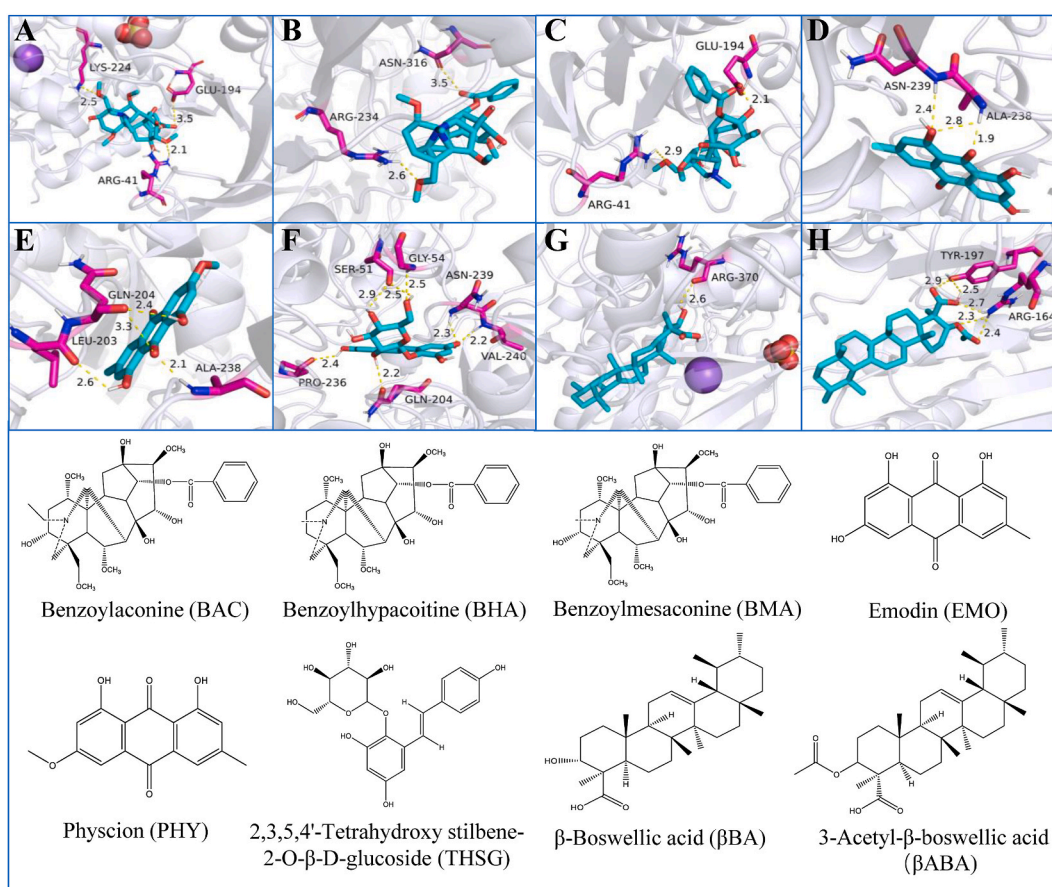


Fig. 4. The structures and molecular docking results of the effective components. (A) BAC-MAPK3, (B) BHC-GAPDH, (C) BMC-MAPK3, (D) EMO-GAPDH, (E) PHY-GAPDH, (F) THSG-GAPDH, (G) β BA-MAPK3, and (H) β ABA-CASP3.

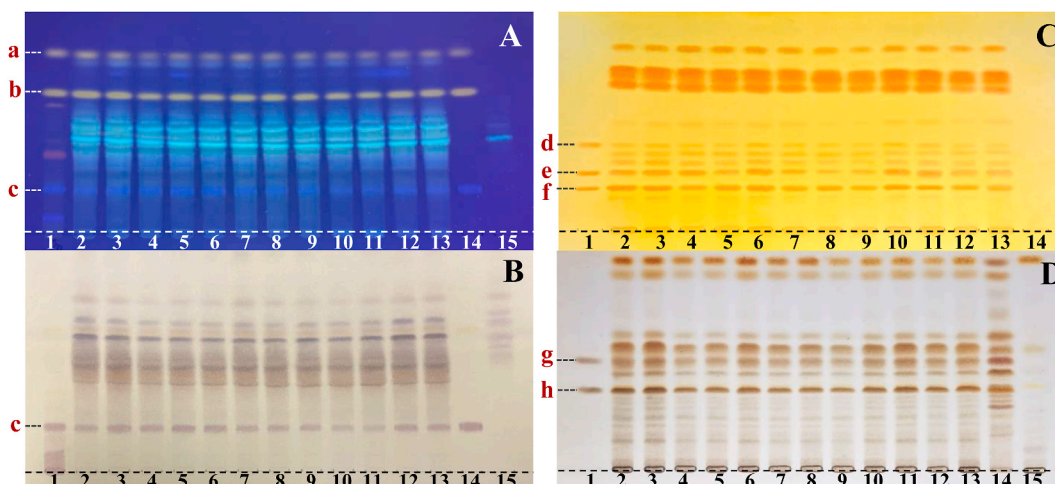


Fig. 5. HPTLC chromatograms of five herbal medicines in SWJPs. (A) HSW, at UV 365, (B) HSW, at sunlight, (C) CW, HCW, and FZ, and (D) RX. (a) PHY, (b) EMO, (c) THSG, (d) BHA, (e) BAC, (f) BMA, (g) β ABA, and (h) β BA. Lanes 2–3, 6, 10–11 were Lot A1–A5. Lanes 4–5, 7–9, and 12–13 were Lot B1–B7. The last lane was negative sample, Lane 1 of A, B and Lane 14 of D were HRS.

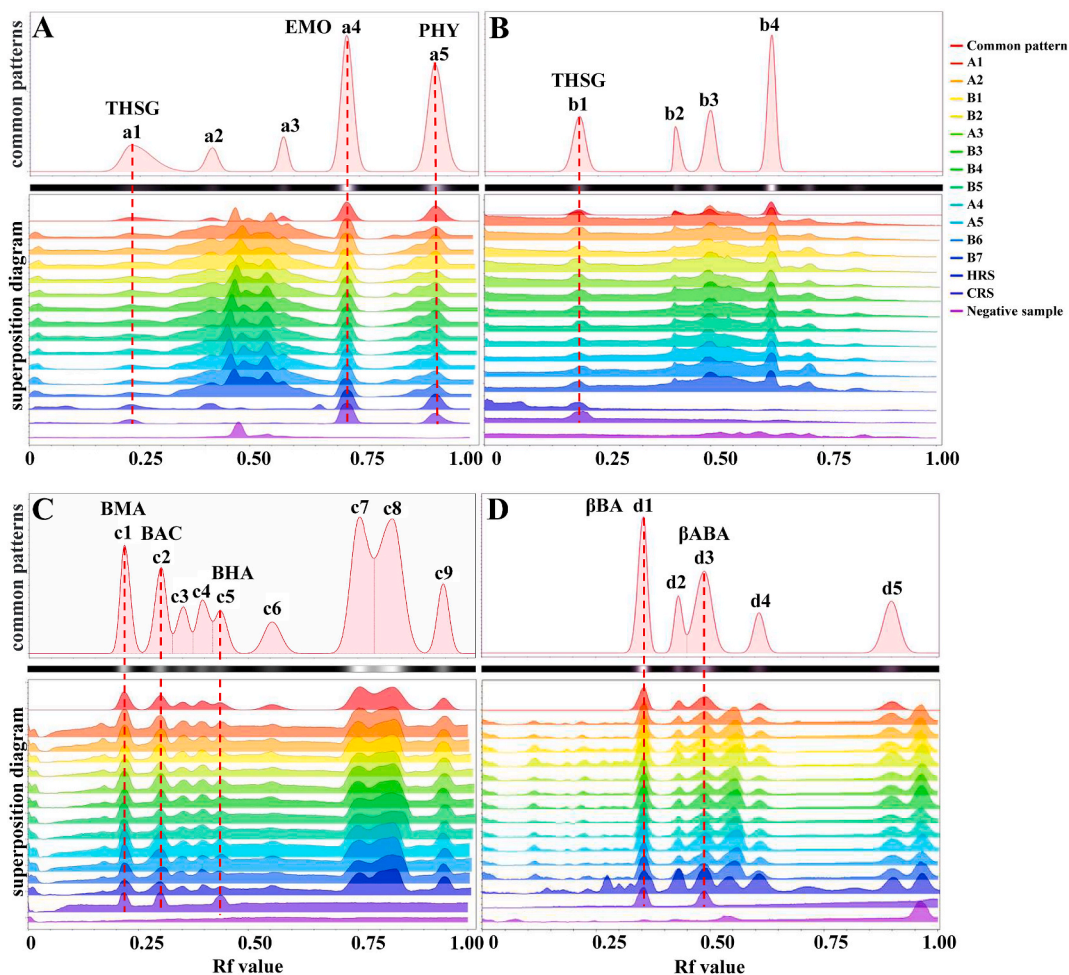


Fig. 6. HPTLC characteristic fingerprints of the five herbal medicines. (A) HSW, at UV 365, (B) HSW, at sunlight, (C) CW, FZ and HCW, (D) RX.

3.5. Establishment of the HPTLC fingerprint

The four HPTLC chromatogram images from the 12 batches of SWJPs were processed using the ChemPattern® software (2020). After multi-color scale scanning and data processing, the interfering fingerprint peaks presenting in the negative sample solutions were subtracted. Subsequently, common patterns and characteristic fingerprints for the different batches of SWJPs were automatically generated (Fig. 6). The fingerprint peaks were numbered from bottom to top according to their ratio shift (Rf) value. These common patterns could be used as reference fingerprint chromatograms for the HPTLC analysis of SWJPs. The results revealed the presence of five common peaks at UV 365 nm and four common peaks in the sunlight for HSW, nine common peaks for CW, HCW, and FZ, and five common peaks for RX. According to the corresponding CRS solutions, eight efficacy components were identified in these common peaks. These reference fingerprint chromatograms (common patterns) for each herbal medicine demonstrated specificity and effectively eliminated interference from other herbal medicines in SWJPs, ensuring the characteristic fingerprinting of SWJPs by HPTLC.

3.6. Validation of HPTLC fingerprint method

The negative samples, which were prepared with any five of the six herbs of SWJPs, did not interfere with the detection of common components (Fig. 5), thereby highlighting the specificity of the method. Moreover, the method had better robustness at 70%–80%, 40%–50%, and 20%–30% humidity and 4–10 °C, 20–25 °C, and 30–35 °C, wherein clear bands of the common components and stable Rf values were observed under these conditions, these changes could not affect the chromatographic behavior. Repeatability analysis revealed that the RSD values of the common peak area of the six samples from CW, HCW, and FZ were 2.94–6.93%, HSW at UV 365 nm and sunlight were 3.53–6.68% and 4.45–6.89%, respectively, and RX was 3.92–6.09% (Table S2). These RSD values were within the acceptance criteria (less than 10%) for repeatability [35].

The thin-layer plates from Qingdao Haiyang Chemical Co., Ltd. (Qingdao, PR China) and Yantai Muxin Glass Products Co., Ltd. (Yantai, PR China) displayed unclear separation of bands, hence, thin-layer plates from Merck were selected for this study as they displayed clear band separation.

3.7. Evaluation of quality consistency

3.7.1. Similarity analysis

The similarities of HPTLC characteristic fingerprints of the 12 batches of SWJPs were analyzed by ChemPattern® software. The results demonstrated that the similarity values among the preparations exceeded 0.9 (Table 3). Specifically, the similarity values for the fingerprints of CW, HCW, and FZ were 0.9561–0.9972, with B2 value being lower. For RX was 0.9283–0.9968, with B3 and B4 being lower. HSW at UV 365 nm and sunlight were 0.9555–0.9985 and 0.9488–0.9996, with B6 and B4 values being lower, respectively. To comprehensively evaluate the similarity of 12 batches of SWJPs by combining all the common peaks data of five herbal medicines fingerprints, the results revealed that all fingerprints peaks were between 0.9765 and 0.9927, with B4 value being lower. Overall, the quality of different batches of SWJPs was stable, although some differences were observed.

3.7.2. Cluster heatmap analysis

To further evaluate the quality consistency of SWJPs, the data from all common peaks across the four HPTLC characteristic fingerprints of the five herbal medicines were integrated and the HPTLC characteristic fingerprints of 12 batches of samples were classified by cluster heatmap analysis (Fig. 7A). The results revealed that the 12 batches of SWJPs were clustered into two categories. Specifically, A4, A3, A5, A1, and A2 were clustered into one group, and B6, B7, B4, B3, B5, B1, and B2 were clustered into the second group. In the second group, the seven samples were further clustered into two subgroups: B6 and B7 formed one subgroup, while B4, B3, B5, B1, and B2 formed the other. This result indicated that the quality of SWJPs produced in June 2020 differed from those produced in July 2020.

Table 3
Similarity analysis results of HPTLC fingerprints of twelve batches of SWJPs.

Batches	HSW fingerprints		CW/HCW/FZ fingerprints	RX fingerprints	All fingerprints
	UV 365 nm	Sunlight			
A1	0.9913	0.9874	0.9795	0.9888	0.9782
A2	0.9843	0.9851	0.9862	0.9954	0.9766
A3	0.9930	0.9564	0.9972	0.9886	0.9844
A4	0.9934	0.9769	0.9883	0.9903	0.9789
A5	0.9944	0.9755	0.9836	0.9900	0.9783
B1	0.9806	0.9996	0.9809	0.9857	0.9927
B2	0.9938	0.9523	0.9561	0.9968	0.9890
B3	0.9985	0.9811	0.9940	0.9283	0.9914
B4	0.9945	0.9488	0.9590	0.9397	0.9765
B5	0.9887	0.9832	0.9785	0.9883	0.9803
B6	0.9555	0.9586	0.9705	0.9953	0.9874
B7	0.9954	0.9987	0.9767	0.9968	0.9866

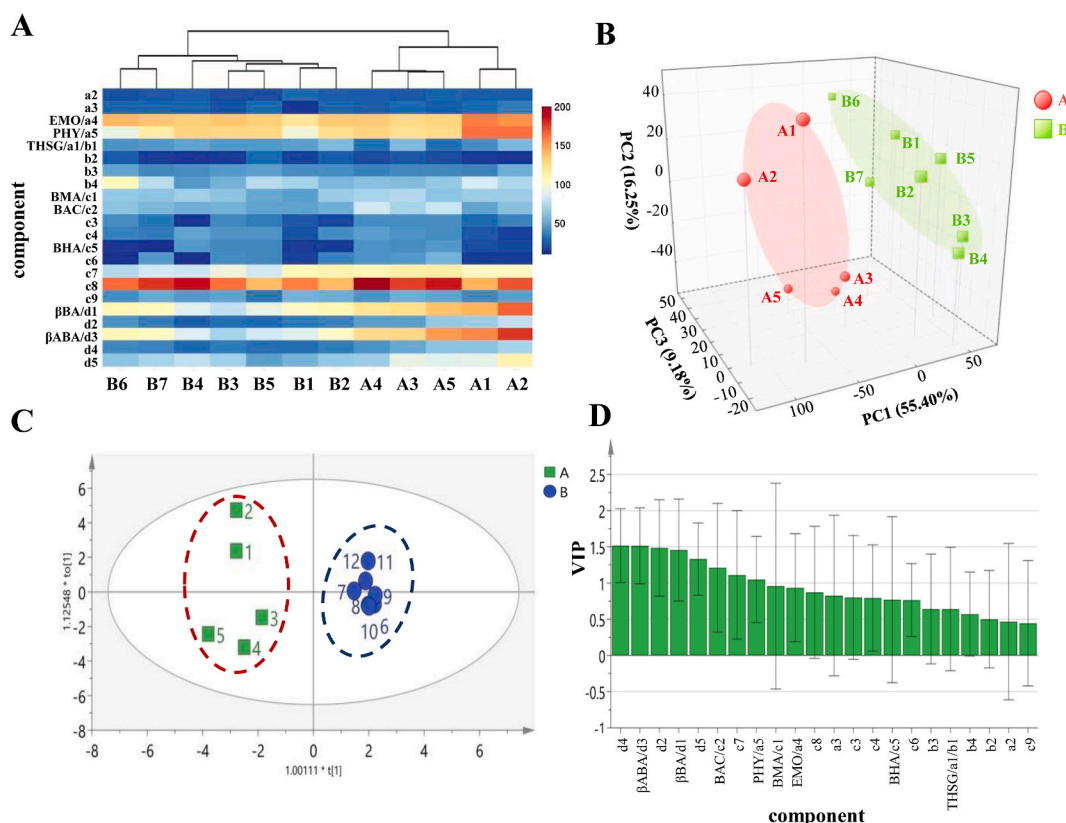


Fig. 7. Quality evaluation of 12 batches of SWJPs based on cluster heatmap, PCA and OPLS-DA analysis. (A) Cluster heat map, (B) PCA's scatter diagram, (C) OPLS-DA's scatter diagram, and (D) VIP value of OPLS-DA. The components represented by the vertical axis of Fig. 7A and the horizontal axis of Fig. 7D are the common peaks of the four HPTLC fingerprints.

3.7.3. PCA analysis

The PCA method was used to analyze the quality differences and consistencies among the 12 batches of SWJPs. PCA is an unsupervised multivariate data analysis approach. It can be used to reduce the dimensionality of multivariate datasets to obtain a new set of variables called principal components [36]. In this study, all the common peak data across the four HPTLC fingerprints of the five herbal medicines were combined and reduced to several principal components for quality evaluation.

The results showed that the contribution rates of the first, second, and third principal components were 55.40 %, 16.25 %, and 9.18 %, respectively, with a cumulative value of 80.83 %. Thus, the three principal components were selected to represent the common peaks' data of the SWJPs. According to PCA's scatter diagram (Fig. 7B), the 12 batches of SWJPs were clustered into two categories. Among them, the batches A1 to A5 of SWJPs, produced in June 2020, were clustered in one category, and batches B1 to B7, produced in July 2020, were clustered in another category. This result was highly consistent with the findings from the cluster heatmap analysis, confirming that PCA is a suitable method for evaluating the quality consistency of complex herbal preparations.

3.8. Components analysis of quality differences

To identify the marker components leading to the quality differences among the 12 batches of SWJPs, all common peak data from the four HPTLC characteristic fingerprints of the five herbal medicines were integrated. Based on the above PCA analysis, SIMCA-P 14.1 software was used for OPLS-DA analysis. The results revealed that the 12 batches of SWJPs were completely consistent with the results of PCA analysis, and they were also clustered into two groups (Fig. 7C). VIP >1 was the standard to screen for components affecting the quality differences in the preparations. According to the VIP diagram (Fig. 7D), the components with a VIP of >1 were d4, β ABA/d3, d2, β BA/d1, and d5 from RX; BAC and c7 from CW, HCW, and FZ; and PHY/a5 from HSW. These key components were identified as the major contributors to the quality variations among the SWJPs batches. Notably, the compositions of RX played a significant role in affecting product quality, suggesting a need for close attention to the quality of RX during production.

3.9. Establishment of quality control limits

Hotelling's T^2 and DMod X control charts were established to monitor the quality of the 12 batches of SWJPs. Hotelling's T^2 and

DMod X are multivariate analysis methods used to detect abnormal fluctuations in products that exceed the control limit. The samples within the control line are considered normal, while those beyond the control line are considered abnormal [37]. Using the SIMCA-P 14.1 software, all the common peak data from the four HPTLC fingerprints of the five herbal medicines were analyzed. Two control charts were drawn (Fig. 8), which illustrated T^2 Crit (99 %) and DCrit (0.05) as the control limits. The upper limits for T^2 Crit and DCrit were 25.64 and 1.67, respectively. In Fig. 7A, T^2 Crit (95 %) was the warning limit, with the upper limit was 14.16. Furthermore, all SWJPs batches fell below the control limit and warning limit. This indicates that although there were minor quality fluctuations among the samples, all of them were normal batches of products with eligible quality.

4. Conclusion

The new strategy based on the multi-color scale and efficacy-oriented HPTLC characteristic fingerprint combined with the chemometric method could be used for the quality evaluation of complex herbal preparations. This strategy identified eight efficacy components within SWJPs for the treatment of RA. Moreover, it enabled the establishment of four HPTLC characteristic fingerprints based on efficacy components, including nine common peaks from HSW, five common peaks from RX, and nine common peaks from CW, HCW and FZ. The quality evaluation results showed that there were differences in the quality of different batches of SWJPs. The key components influencing the quality consistency primarily included eight components such as β ABA, β BA, BAC, PHY. Additionally, this study successfully established quality control limits for the preparation. Compared to other chromatographic fingerprinting methods, this strategy offers simplicity, speed, and cost-effectiveness. In particular, the HPTLC method allows for qualitatively identification and quality evaluation of the preparation simultaneously. Notably, it is the first time that this strategy has been applied to the quality evaluation of complex herbal preparations. It holds valuable implications for quality control in the production process, intermediate products, and final products of herbal preparations. This strategy is expected to be helpful for the quality control of other complex herbal preparations.

Funding

This project was funded by Science and Technology Planning Project of Yunnan Provincial Science and Technology Department (NO. 20202AA100004-3), National Natural Science Foundation of China (NO. 82374139), the Traditional Chinese Medicine Bureau of Guangdong Province (NO. 20232037) and the Macau Science and Technology Development Fund (No. 0122/2020/A).

Ethics declarations

Review and/or approval by an ethics committee was not needed for this study because we did not conduct any animal or human experiments.

CRedit authorship contribution statement

Pei Wenhan: Data curation, Formal analysis, Investigation, Methodology, Validation, Visualization, Writing – original draft. **Yufeng Huang:** Data curation, Formal analysis, Investigation, Methodology, Validation, Visualization. **Yuan Qu:** Data curation, Formal analysis, Investigation, Methodology, Validation, Visualization. **Xiuming Cui:** Data curation, Formal analysis, Investigation, Methodology, Validation, Visualization. **Liqin Zhou:** Resources. **Hongfang Yang:** Resources. **Mingshun Zhao:** Resources. **Zhifeng Zhang:** Conceptualization, Funding acquisition, Resources, Supervision, Writing – review & editing. **Fan He:** Conceptualization, Funding acquisition, Resources, Supervision, Writing – original draft. **Hua Zhou:** Conceptualization, Funding acquisition, Resources, Supervision, Writing – review & editing.

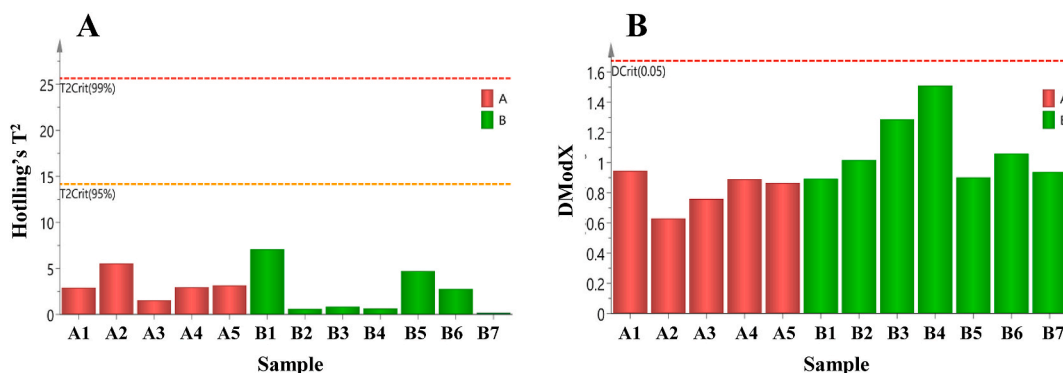


Fig. 8. Quality control chart of 12 batches of SWJPs: (A) Hotelling's T^2 control chart, and (B) DModX control chart.

Declaration of competing interest

Liqin ZHOU, Hongfang YANG, Mingshun ZHAO are the employees of Yunnan Jinwu Black Medicine Pharmaceutical Co. Ltd. who donated Sanwujiào Pill samples for this research, but had no role in the data acquisition, statistical analysis and writing of this article. The other authors declare that they have no known competing financial interests or personal relationships that could have appeared to influence the work reported in this paper

Acknowledgements

The authors are grateful to Runtao Tian and Haodong Xu of Chemmind (Beijing) Technologies, Co. Ltd for their kind technical support of image and data processing of HPTLC to this study.

Appendix A. Supplementary data

Supplementary data to this article can be found online at <https://doi.org/10.1016/j.heliyon.2023.e22098>.

References

- [1] F. Cheung, TCM: made in China, *Nature* 480 (7378) (2011) S82–S83.
- [2] L.C. Klein-Junior, M.R. de Souza, J. Viaene, T.M.B. Bresolin, A.L. de Gasper, A.T. Henriques, Y.V. Heyden, Quality control of herbal medicines: from traditional techniques to state-of-the-art approaches, *Planta Med.* 87 (12–13) (2021) 964–988.
- [3] L. He, Y. Liu, K. Yang, Z. Zou, C. Fan, Z. Yao, Y. Dai, K. Li, J. Chen, X. Yao, The discovery of Q-markers of Qiliqiangxin Capsule, a traditional Chinese medicine prescription in the treatment of chronic heart failure, based on a novel strategy of multi-dimensional "radar chart" mode evaluation, *Phytomedicine* 82 (2021), 153443.
- [4] X. Lu, Y. Jin, Y. Wang, Y. Chen, X. Fan, Multimodal integrated strategy for the discovery and identification of quality markers in traditional Chinese medicine, *J Pharm Anal* 12 (5) (2022) 701–710.
- [5] Y.J. Zhang, Y.Y. Jiang, Research approach and progress in term of the quality of Chinese medicinal, *Acta Chin Med Pharm* 49 (7) (2021) 106–112.
- [6] J. Han, K. Xu, Q. Yan, W. Sui, H. Zhang, S. Wang, Z. Zhang, Z. Wei, F. Han, Qualitative and quantitative evaluation of Flos Puerariae by using chemical fingerprint in combination with chemometrics method, *J Pharm Anal* 12 (3) (2022) 489–499.
- [7] X. Fan, T. Hong, Q. Yang, D. Wang, J. Peng, W. Xiao, X. Yang, X. Hu, C. Yu, S. Du, J. Bai, Quality assessment of fried licorice based on fingerprints and chemometrics, *Food Chem.* 378 (2022), 132121.
- [8] M. Liao, H. Shang, Y. Li, T. Li, M. Wang, Y. Zheng, W. Hou, C. Liu, An integrated approach to uncover quality marker underlying the effects of *Alisma orientale* on lipid metabolism, using chemical analysis and network pharmacology, *Phytomedicine* 45 (2018) 93–104.
- [9] Z. Chen, M. Wang, Y. Yang, X. Cui, J. Hu, Y. Li, F. Zhao, Promotion of a quality standard for *Porana sinensis* Hemsl. based on the efficacy-oriented Effect-Constituent Index, *Biomed. Chromatogr.* 34 (2) (2020), e4726.
- [10] H. Zhang, S. Li, H. Feng, M. Li, Z. Pei, T. Kang, Quality control of Shuanghuanglian preparations using an effect-constituent index, *Acta Pharm. Sin. B* 54 (12) (2019) 2149–2154.
- [11] USFDA, FDA Guidance for Industry-Botanical Drug Products (Draft Guidance), US Food and Drug Administration, Rockville, MD, USA, 2000, pp. 18–22.
- [12] EMA, Guideline on Quality of Herbal Medicinal Products/Traditional Herbal Medicinal Products, Committee on Herbal Medicinal Products, HMPC) European Medicines Agency, London, UK, 2011.
- [13] NMPA, Technical Requirements for Fingerprint Study of Traditional Chinese Medicine Injections, National Medical Products Administration, 2005.
- [14] C.J. Zhan, H. Wang, Y. Wang, Quality evaluation of *Atractylodes macrocephala* rhizoma through fingerprint qualitative analysis and quantitative analysis of multi-components by single marker, *J. Pharm. Biomed.* 219 (2022).
- [15] I.M. Simion, D. Casoni, C. S'arbu, Multivariate color scale image analysis-Thin layer chromatography for comprehensive evaluation of complex samples fingerprint, *J. Chromatogr. B.* 1170 (2021), 22590.
- [16] S. Tian, H. Guo, M. Zhang, H. Yan, X. Wang, H. Zhao, Rapid authentication of *Chaenomeles* species by visual volatile components fingerprints based on headspace gas chromatography-ion mobility spectrometry combined with chemometric analysis, *Phytochem. Anal.* 33 (8) (2022) 1198–1204.
- [17] A. Kamboj, A.K. Saluja, Development of validated HPTLC method for quantification of stigmasterol from leaf and stem of *Bryophyllum pinnatum*, *Arab. J. Chem.* 10 (2017) S2644–S2650.
- [18] A.K. Goswami, N. Gogoi, A. Shakya, H.K. Sharma, Development and validation of high-performance thin-layer chromatographic method for quantification of berberine in rhizomes of *Coptis teeta* wall, an endangered species collected from Arunachal Pradesh, India, *J. Chromatogr. Sci.* 57 (5) (2019) 411–417.
- [19] Ministry of Health, PRC, Formulation of traditional Chinese medicine, Pharmaceutical Standard of Ministry of Health of the People's Republic of China 20 (1992). Z20-11.
- [20] S.D. Jiang, Effect and Mechanism of Sanwujiào Pills on Fibroblast-like Synovial Cells in Rheumatoid Arthritis, Kunming University of Science and Technology, 2022.
- [21] Q. Li, L.N. Guo, J. Zheng, Reaserch progress of medicinal genus *Aconitum*, *Chin. J. of Pharm. Anal.* 36 (7) (2016) 1129–1149.
- [22] H. Sun, Y. Liang, H.J. Zhang, Y.Q. Fan, W.W. Sun, Research progress of *Polygonum multiflorum*, *Occup. Health* 35 (17) (2019) 2436–2441+2445.
- [23] M.Z. Siddiqui, *Boswellia serrata*, a potential anti-inflammatory agent: an overview, *Indian J. Pharm. Sci.* 73 (3) (2011) 255–261.
- [24] Y. Jin, Chemical Constituents from Rhizome of *Typhonium Giganteum* Engl. And Their in Vitro Neuroprotective Activities, Nanjing Medical University, 2016.
- [25] C.Q. Luo, Studies on Quality Standard and Pharmacokinetics of Sanwujiào Pills in Vivo, Kunming University of Science and Technology, 2022.
- [26] C.Q. Luo, S.Y. Xiao, D. Lv, Y. Qu, X.M. Cui, L.H. Duan, Study on HPLC fingerprint and multi-indicator quantitative analysis of Sanwujiào, *J. Yunnan Univ. Nat. Sci. Ed.* 44 (1) (2022) 150–159.
- [27] Y.X. Guan, Q. Mei, J. Cheng, Determination of 2,3,5,4'-Tetrahydroxystilbene-2-O-β-D-Glucoside in Sanwujiào Pills by HPLC, *China Pharmacist* (9) (2008) 1055–1057.
- [28] K.Y. Hsin, S. Ghosh, H. Kitano, Combining machine learning systems and multiple docking simulation packages to improve docking prediction reliability for network pharmacology, *PLoS One* 8 (12) (2013), e83922.
- [29] C.X. Wei, Y.X. Zheng, X. Zhou, J.L. Diao, Xiaoe huanglong granules in the treatment of attention-deficit hyperactivity disorder based on network pharmacology and molecular docking, *Chinese Pharm* 32 (5) (2023) 72–79.
- [30] ICH guidelines, validation of analytical procedure. <https://www.ich.org/page/quality-guidelineswww.nihs.go.jp>.
- [31] J. Kong, X.S. Yang, X.L. Huang, X.P. Wang, H.M. Wu, Study on thin layer chromatography identification of *Polygoni Multiflori Radix* and its counterfeit from different areas, *Lishizhen Med. Mater. Med. Res.* 31 (6) (2020) 1374–1376.

- [32] Y.H. Hu, S.M. Yuan, J. Yang, Study on quality control of xuetong capsule, *J. Tradit. Chin. Med.* 51 (8) (2017) 98–102.
- [33] F.C. Zhao, J. Li, Recent progress in research of alkaloid in Aconitum plants, *Chin. J. Mod. Appl. Pharm.* 27 (S1) (2010) 1177–1182.
- [34] L. Xia, Z.Q. Song, L.L. Zhang, Z. Wei, Y.N. Cao, Z.L. Liu, Identification of boswellic acids in Olibanum and Chinese herbal preparation containing Olibanum by thin layer chromatography, *J. Tradit. Chin. Med.* 34 (7) (2012) 1403–1404.
- [35] E. Guzelmeric, I. Vovk, E. Yesilada, Development and validation of an HPTLC method for apigenin 7-O-glucoside in chamomile flowers and its application for fingerprint discrimination of chamomile-like materials, *J. Pharm. Biomed. Anal.* 107 (2015) 108–118.
- [36] L.N. Liu, H.Y. Jin, Z. Ke, W.Y. Xu, L. Sun, S.C. Ma, A strategy for quality control of ginkgo biloba preparations based on UPLC fingerprint analysis and multi-component separation combined with quantitative analysis, *Chin. Med.* 17 (1) (2022) 72.
- [37] Y.Z. Hou, P. Li, H.M. Xiao, J.L. Chen, Z. Li, W.L. Li, Determination of saponins in Xuesaitong Drop Pills and study on batch consistency evaluation, techniques , *Zhong Cao Yao.* 50 (11) (2019) 2552–2559.